Propeller-Wing Integration on the Parallel Electric-Gas Architecture with Synergistic Utilization Scheme (PEGASUS) Aircraft

Nathaniel J. Blaesser*
Aeronautics Systems Analysis Branch, NASA Langley Research Center

Electrically powered aircraft show promise for reducing emissions and energy consumption, but many of the opportunities surrounding electric propulsion have yet to be explored. One opportunity is the use of multiple propulsors or distributed propulsion for improved propulsion-airframe integration. However, the size, power, location, and optimum number of propulsors has not been thoroughly vetted. This paper describes the use of FlightStream, a surface vorticity solver, to investigate the aerodynamic-propulsion integration of four propulsors across the leading edge of a wing, two inboard and two at the wingtips, as proposed in the NASA Parallel Electric-Gas Architecture with Synergistic Utilization Scheme (PEGASUS) concept. FlightStream was used to determine the minimum power required for cruise for the PEGASUS aircraft. The study found that tip propellers are effective at lowering both viscous and induced drag when compared to inboard propellers alone or inboard propellers combined with tip propellers. Despite this drag savings, the propulsive efficiency was reduced when a single propeller class was used, resulting in a higher system power consumption when compared with using multiple propeller classes. Reductions in propeller efficiency are related to increases in disc and blade loading of the propeller; thus, larger propellers or higher tip speeds are seen as possible means of to improve system performance.

Nomenclature

C_D	=	Coefficient of drag
C_{D0}	=	Zero-lift coefficient of drag
C_{Di}	=	Coefficient of induced drag
C_L	=	Three-dimensional coefficient of lift
C_T	=	Coefficient of thrust
D	=	Propeller Diameter
n	=	Revolutions per second
P'	=	Power without boundary layer ingestion
P_{BLI}	=	Power with boundary layer ingestion
P_{shaft}	=	Shaft power
T	=	Thrust
V	=	Velocity
$\boldsymbol{x}$	=	Optimization variables
α	=	Angle of attack
ρ	=	Freestream air density
η	=	Spanwise propeller position
η_p	=	Propeller efficiency
$(\cdot)_t$	=	Target values

*Aerospace Engineer, Aeronautics Systems Analysis Branch, 1 N. Dryden Street MS 442, Hampton VA, Member

I. Introduction

Electric propulsion has created a new design space for potential aircraft concepts. The current paradigm is that fewer, larger propulsors are advantageous over numerous, smaller propulsors. Electric motors are largely scale independent, which allows for different combinations of motors in terms of number, size, and location. Further, the power generation of a turbine can exist independently from the thrust-producing propeller or fan. With this new design space, additional tools and analysis approaches are required to take advantage of mutual propulsion and aerodynamic benefits that may exist in various architectures and concepts.

To explore the new opportunities for subsonic transports, in which propulsor number is not minimized and the propulsors can be placed in strategic locations, NASA's Aeronautics Systems Analysis Branch created the Parallel Electric-Gas Architecture with Synergistic Utilization Scheme (PEGASUS) aircraft [1, 2]. PEGASUS uses wingtip propulsors as the primary cruise propulsion source, which are aided by a tail propulsor during cruise and two inboard propulsors during takeoff. Each propulsor class provides a specific function: the aft propulsor re-energizes the fuselage's boundary layer, the wingtip propulsors reduce induced drag while providing cruise thrust, and the inboard propulsors supplement the wingtip propulsors during takeoff and climb.

PEGASUS, shown in Fig. 1, is a 48-passenger aircraft based on the ATR-42-500 with a targeted entry in service (EIS) date of 2030. The nominal mission includes a 400 nautical mile cruise below transonic speeds, around Mach 0.5, at an altitude of 20,000 ft. This aircraft class was selected for the PEGASUS architecture because a regional aircraft has a higher likelihood of implementing a battery-powered hybrid-electric architecture due to its relatively small size. The current state of battery technology is such that adding additional electrical power considerably adds to the maximum takeoff weight of the aircraft. Thus a smaller aircraft, like PEGASUS, will incur a smaller weight penalty for electrification than a larger, 150 passenger class aircraft. Even at a smaller size, PEGASUS will require gas turbines to generate at least a portion of the required power without significant advances in battery technology. As such, the current incarnation of PEGASUS includes parallel hybrid gas-electric turbines at the wingtips. The inboard and aft propellers are driven solely by battery-powered electric motors.

Fig. 1 Artist's rendering of PEGASUS.

Past studies have investigated the preliminary design aspects of PEGASUS [1, 2]. In particular, these past studies highlighted the need for more capable tools to investigate advanced concepts such as PEGASUS, as well as how challenging the reserve mission is for a hybrid-electric aircraft. The need to realize every efficiency benefit, combined with the option of using multiple propulsors to achieve the target thrust, led to the requirement for a higher fidelity propulsion-airframe integration (PAI) study.

Section II focuses on the key physics of propeller-wing interaction as well as some of the past studies that have addressed this topic. Section III describes the tools and methods to perform the analysis, the specific operating conditions, and the design space considered. The results are summarized in Section IV, with the overarching trends highlighted and discussed.

II. Background

The PEGASUS architecture has three propellers providing cruise thrust, one tractor propeller located at each wingtip and one pusher propeller at the aft of the fuselage, with two inboard tractor propellers to supplement thrust on takeoff, as shown in Fig. 2. The idea behind this approach is that the wingtip propellers will counteract the wingtip vortex and reduce induced drag on the aircraft. Although the envisioned scenario has the inboard propellers folded at cruise, realistic scenarios exist in which using a combination of inboard and tip propellers could provide distinct benefits. For example, using the electric inboard motors to supplement the tip engines could reduce emissions or fuel burn. However, using all these propellers can significantly influence the system performance of the aircraft.

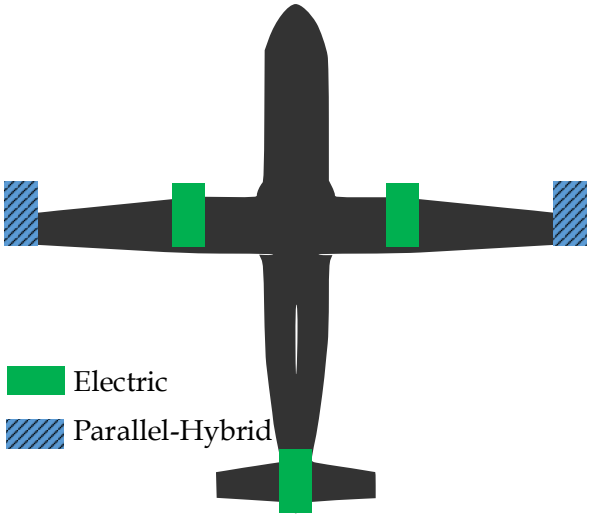

Fig. 2 PEGASUS's propulsion architecture

One of the goals of this study is to quantify these PAI effects. The focus of this paper is the wing propulsors, with the aft propulsor not explicitly modeled except through a power saving coefficient (PSC). The PSC defined in Equation 1 is used in place of the aft propulsor [3], where P' is the power required without a boundary layer ingestion (BLI) propulsor and P_{BLI} is the power with a BLI propulsor. The design space becomes the diameter of the inboard and tip propellers, the helical propeller tip Mach number of each propeller, and the fraction of cruise thrust provided by the inboard propellers (with the tip propellers providing its compliment).

$$PSC = \frac{P' - P_{BLI}}{P'} \tag{1}$$

Numerous studies have been conducted on the performance of propellers and their interaction with nearby wings. Kroo [4] focused on the propeller's impact on the lift distribution, finding that the greater the change in lift distribution from elliptic, the higher the system drag. Via this reasoning, Kroo found that spinning the propeller inboard-up was preferable to outboard-up. Veldhuis investigated moving the propeller along all three axes of the wing [5]. Veldhuis found modest changes when moving the propeller in the streamwise-direction, but a significant savings by moving the propeller toward the tip. Veldhuis also found that the vertical position can have a significant influence, provided the propeller's induced velocity is high. Specifically, moving the propeller higher increased the C_L of the wing, as more flow was accelerated over the top of the airfoil. This lift benefit came with a corresponding drag penalty as well. Miranda and Brennan used an internally developed tool to run parametric studies of wingtip propellers [6]. Their results demonstrated that smaller, slower spinning propellers reduced total power consumption for a given configuration. The authors note that this leads to highly loaded propellers, but propeller efficiency was not considered when determining the power required.

When considering the benefits of reduced induced drag, it is important to consider how much drag can be reduced. An aircraft's maximum lift-to-drag ratio is achieved when the induced drag is equal to the viscous drag. While aircraft may not always operate at the max lift-to-drag ratio, one can assume that the induced drag constitutes a maximum of half of the total drag. Thus even a 20% reduction in induced drag would lead to modest total drag reductions.

To compliment the reduction in induced drag achieved by wingtip propellers, wingtip propellers can also enable greater laminar flow over a wing. The flow behind a propeller, barring advanced active flow control, will be turbulent. Therefore, even if the ATR-42-500 used a natural laminar flow (NLF) wing, the propeller wash would cause nearly 1/3 of the wingspan to be fully turbulent. By making half of the propeller diameter to extend beyond the wingtip, the amount of turbulent flow across the wing can be dramatically reduced. Because this benefit is only realized for a laminar flow wing, there exists a synergy between wingtip propellers and NLF wings.

The investigation uses FlightStream, a surface vorticity solver developed by Research in Flight [7]. FlightStream can analyze three-dimensional geometries and is designed to perform powered aerodynamic simulations. This makes FlightStream ideally suited for handling propeller-wing interactions. Figure 3 shows the geometry for this investigation within FlightStream. FlightStream is only capable of analyzing subsonic flows, though it does have several compressibility factors for moderately transonic flows. FlightStream contains a uniformly loaded actuator disk model based on Conway's method [8], which permits the calculation of swirl aft of the propeller suitable for conceptual design. This feature enables the solver to calculate the local effect of the propeller on the wing, as required for this investigation. FlightStream is unable to analyze the effect of the wing on the propeller, but for a tractor configuration, this effect is much smaller than the propeller's effect on the wing. Recent studies have employed FlightStream in a similar approach [9, 10].

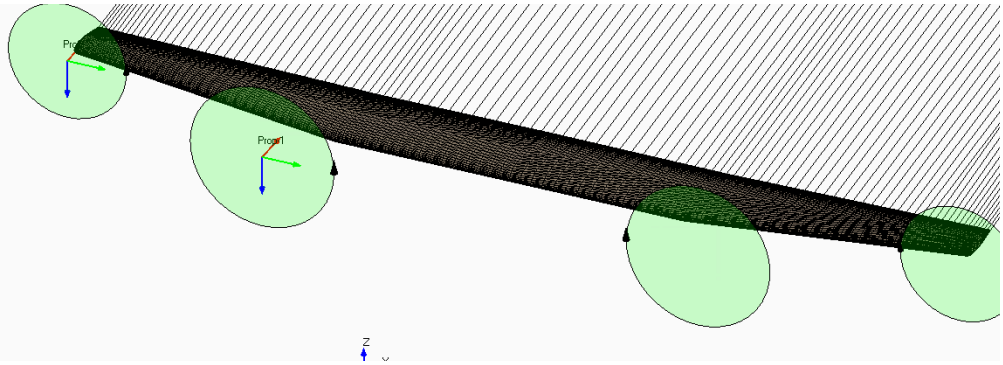

Fig. 3 FlightStream's user interface with the PEGASUS wing.

III. Approach

A. Validation

Prior to implementing FlightStream, the tool was validated against Veldhuis's data. The specific validation case consists of a rectangular wing with a chord of 0.785 ft, a semispan of 2.10 ft, and a NACA 64_2-A015 airfoil as seen in Fig. 4. The propeller has a diameter of 0.775 ft and is located in line with the quarter chord vertically. For this study, the wing is positioned at an angle of attack of 4.2°, though the propeller is normal to the freestream. The advance ratio is 0.92, the coefficient of thrust, C_T, is 0.127 and the propeller rotates with an inboard-up direction. Not provided in Veldhuis's papers are the freestream velocity or atmospheric conditions. For this analysis, the freestream conditions were assumed to be 50 m/s at sea level standard conditions.

Prior to assessing the validation data, it is worth noting that a perfect validation is not possible for several reasons. The primary reason is that the tools used, surface vorticity and flat plate drag approximations, do not solve the full set of governing equations. The second reason is that the experimental setup is not fully described; for example, the propeller geometry is not given, thus the thrust distribution cannot be known. The propeller is likely not a uniformly loaded propeller, which is the only type that FlightStream is able to model.

Figure 5 shows the validation data, with Fig. 5a comparing C_L and 5b comparing C_D as the propeller moves toward the wingtip. The computational model agrees moderately well with the experimental data, and the trends are largely correct. As the propeller moves toward the wingtip, the C_L increases, as expected. The experiment predicts a peak increase of around 11%, whereas FlightStream predicts a peak increase of 4%. The difference is negligible until the propeller begins to extend beyond the wingtip, and the general trend is correct. The one exception is the wingtip, where FlightStream predicts the C_L to begin declining. The source of this discrepancy is difficult to identify, but possibile sources are the hub of the propeller is not being modeled and the use of a uniformly loaded actuator disk. Both of these

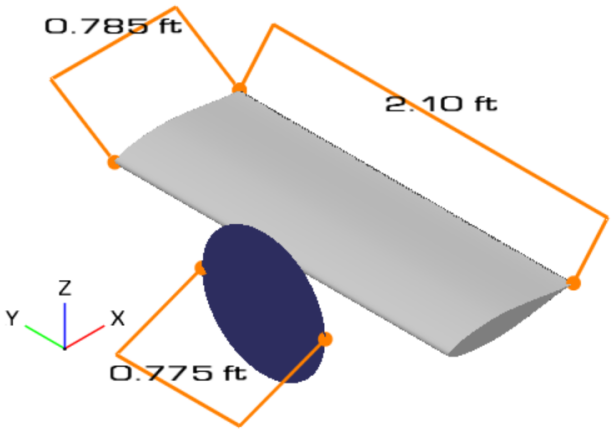

Fig. 4 Validation test setup based on Veldhuis's data. The spanwise location of the propeller varies with the test.

simplifications place the propeller slipstream closer towards the center of the propeller compared to a real propeller. A hub will concentrate the slipstream into a smaller area, while a radially varying slipstream places the maximum induced flow at approximately 75% of the propeller radius. Therefore, even when the propeller is centered at the wingtip, most of the induced velocity will be more inboard on an actual propeller with a hub, than a uniformly loaded propeller without a hub.

Comparing the drag numbers required more post-processing. FlightStream is capable of modeling flow transition, in addition to assuming the flow is entirely laminar or turbulent. The Reynolds number for this scenario is low enough that, when unblown, most of the wing has laminar flow. However, aft of a propeller the flow will not be laminar, regardless of Reynolds number. To account for this, the laminar and turbulent C_D were calculated in FlightStream, and the final C_D estimate was calculated by considering the wing behind the propeller to be turbulent and the rest to be laminar. This approach means that as the propeller extends beyond the wingtip, the amount of turbulent flow decreases. This reduction in viscous drag, C_{D0}, combined with the reduction in induced drag, C_{Di}, from the propeller counteracting the wingtip vortex, yields a reduction in drag similar to that observed by Veldhuis. Figure 5b shows the percent total drag reduction (induced and viscous) for a propeller location, as compared to the most inboard location for both the experimental and numerical investigations. Using this approach, there is surprisingly good overlap between the computation and experimental results. One should interpret this as FlightStream successfully capturing the trend, rather than it being able to accurately predict the absolute drag value.

B. Analysis Parameters

The outer mold line of PEGASUS is based on the ATR-42-500. By searching open literature, much of the geometry of the aircraft and airfoil can be reverse engineered to a suitable degree [11–13]. As such, a notional geometry for PEGASUS was generated in OpenVSP [14]. The wing planform matches that of the ATR-42-500, but the wing has not been optimized for minimum drag (induced or otherwise) via controlling the twist distribution or other means.

The wingtip propeller diameter was a variable within the tradespace, but there are upper limits to the propeller's diameter, independent of its performance, one of which is wingtip strike during a crosswind landing. Crosswind landings necessitate either a crab approach or a slideslip approach. The amount of crabbing or sideslip angle varies with approach speed and crosswind, but Raymer recommends extending a line from the landing gear out five degrees, with an additional six inches margin [15]. Graphically, this is illustrated in Fig. 6. Based on the ATR-42-500 geometry, this limits the tip propeller diameter to 19 ft, which is considerably larger than the 13 ft inboard propellers. There are other constraints that will influence propeller diameter, in particular mass and structural aspects, which will likely drive the diameter below the 19 ft estimate; however, for this analysis, the maximum propeller diameter was set according to the 19 ft limit imposed by crosswind landings.

For this analysis, the wing was isolated from the fuselage and engine nacelles, then imported into FlightStream, as previously shown in Fig. 3. The powered boundary conditions were controlled through the propeller's coefficient of thrust, C_T, and revolutions per minute (rpm). Equation 2 gives the definition of C_T, as used in FlightStream, where T is

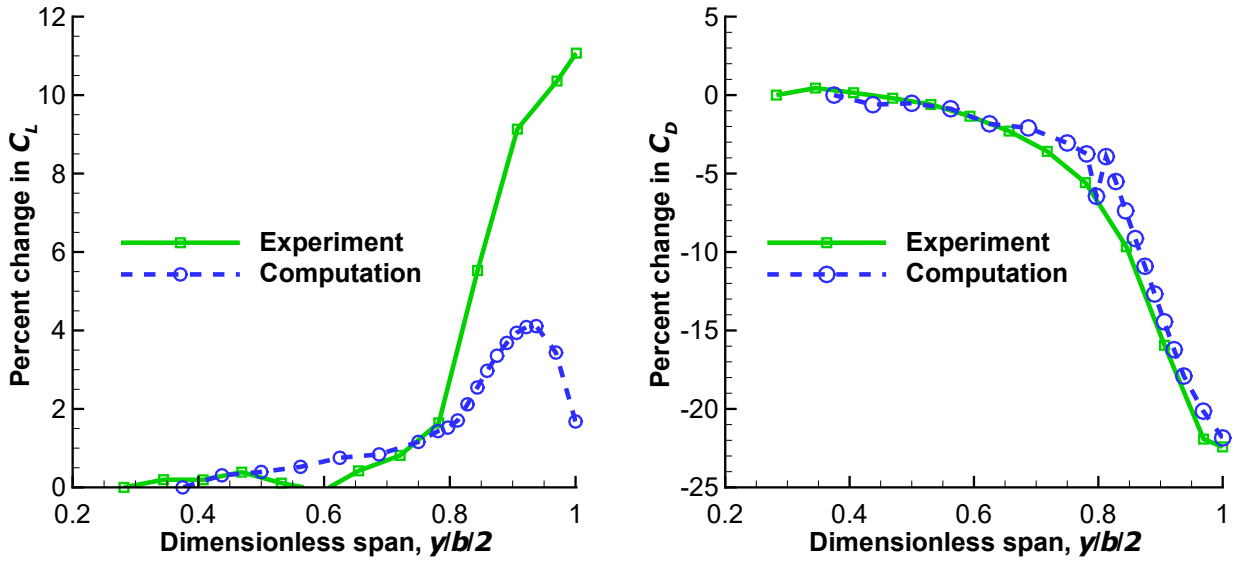

(a) Lift comparison. **(b) Drag comparison.**

Fig. 5 Validation against experimental data from Veldhuis [5]. The percent change is relative to the functional when the propeller is at its most inboard location.

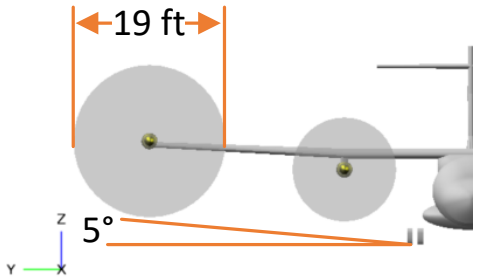

Fig. 6 The requirements for preventing a tip strike in a cross wind landing can still accommodate a large wingtip diameter propeller.

the thrust, ρ is the freestream density, n is the propeller's rotational velocity in revolutions per second, and D is the propeller diameter.

$$C_T = \frac{T}{1/4\rho\pi^3 D^4 n^2} \tag{2}$$

Drag is one metric of a wing's performance, but for integrated PAI, system power is a better metric [16]. To convert from required thrust to consumed power, one must use a propeller model and calculate a propeller efficiency, η_p, defined in Eq. 3, where P_{shaft} is the shaft power provided by the engine and V is the freestream velocity.

$$\eta_p = \frac{TV}{P_{\text{shaft}}} \tag{3}$$

To model a propeller, the flight conditions and propeller specific information are input into XROTOR, a propeller analysis code developed by Mark Drela and Harold Youngren [17]. XROTOR calculates the performance of a minimum induced loss (MIL) propeller, including its efficiency. Table 1 lists the inputs required by XROTOR for propeller design common to the inboard and wingtip propellers. Though XROTOR requires inputs in metric units, Imperial units are listed. Many of these values are estimates that reflect the early stage of development for PEGASUS. For example, the ATR-42-500 has a six-bladed propeller, which is kept for PEGASUS, on both the wingtip and inboard propeller. The propeller hub and its wake displacement is set to be 1/10 of the propeller diameter, and the rpm is calculated such that

the helical tip Mach number is held at a certain value. The blade sectional lift coefficient is dependent on the airfoil used for the propeller. At this point, no actual airfoil has been selected, therefore a lift coefficient of one is used as a reasonable estimate.

Table 1 Inputs for XROTOR's Propeller Design Feature

Parameter	Units	Value
Altitude	ft	20000
Blades	[-]	6
Airspeed	kts	291
Blade sectional lift coefficient	[-]	1

Fundamentally, the goal is to minimize required power during cruise at 20,000 ft at a freestream Mach number of 0.48. The constraints are that the wing must maintain a target lift coefficient and that the aircraft thrust must balance with the drag. This study is power source agnostic, the model does not place an emphasis on whether the power is generated by burning fuel or is provided by batteries. The information from this study may be used to make decisions on where the power should come from, but that step is left as future work.

Mathematically, the optimization is described via Eq. 4. The target lift coefficient, $C_{L,t}$, is set to 0.5, which is representative of an actual cruise C_L. The model only includes the aircraft wing and propellers, thus the viscous drag for the rest of the aircraft is included as a constant value of 200 counts. This value comes from estimates in FLOPS [18].

$$\begin{aligned} \underset{\boldsymbol{x}}{\text{minimize}} \quad & P_{\text{shaft}}(\boldsymbol{x}) \\ \text{subject to} \quad & C_L(\boldsymbol{x}) = C_{L,t}, \\ & C_D(\boldsymbol{x}) = C_{D,t} \end{aligned} \tag{4}$$

The angle of attack and total thrust are the primary variables to control to meet the constraints. Other possible design variables within the optimizer include propeller diameter, tip speed, power saving coefficient, and inboard propeller placement. Figure 7 shows the workflow for the framework, where $\boldsymbol{x}$ is a vector of design variables, typically angle of attack and thrust. The framework is modular such that design variables can be added, removed, or exchanged quickly depending on the analysis goals.

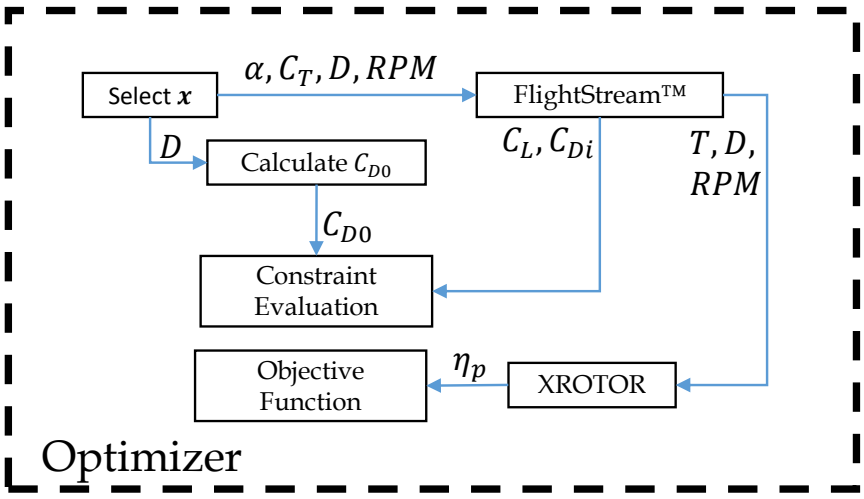

Fig. 7 Workflow for the analysis.

IV. Results

A. Effect of Tip Propeller Diameter

The first parametric study investigated the effect of tip propeller diameter on cruise thrust and power required. The inboard propeller was assumed to be folded and did not contribute to the propulsive thrust. Thus the wing area inboard of the tip propellers was assumed to be laminar. Figure 8 shows the thrust required for balanced flight and the power required from a MIL propeller to produce that thrust. The analysis was performed for two PSC values (10% and 20%) and two tip Mach numbers, 0.7 and 0.8. The first trend, common to all scenarios, is that increasing the tip diameter increases the thrust required but decreases the power required. There are two reasons for the thrust trend. The first is that increasing the tip diameter increases the blown and turbulent area of the wing, which increases viscous drag. Second, the induced drag increases with propeller diameter because the rotational flow from the propeller is less concentrated; however, the induced drag is still lower with a propeller than without. The next trend is the effect of tip Mach number, which has little effect on the thrust required to balance drag but has a significant effect on the power required. The thrust is likely similar because lowering tip speed increases the induced drag relative to a high tip speed, but the scrubbing drag is lower. The power is much higher because spinning a propeller slower effectively raise the disc loading of the propeller. The effect of disc loading will be discussed shortly. It is worthwhile to revisit Miranda's results, which stated that slower and smaller diameter propellers have the lowest drag. This analysis agrees that reducing propeller diameter lowers the aircraft drag; however, the tip Mach number had little effect. The final trend to analyze is the effect of PSC. This analysis does not include the power consumed by the aft propulsor, so increasing the PSC reduces the load carried by the wingtip propulsors. From Fig. 8, it appears that PSC simply shifts the power curves downward, but closer examination also reveals that increasing PSC flattens the curve of power versus diameter. This flattening is also a function of disc loading on the propeller and its related propeller efficiency.

B. Effect of Disc Loading

Disc loading is a simplified model for propellers wherein the propeller load (thrust) is divided by the swept area of the blade. Propellers are essentially rotating wings, thus higher disc loading is equivalent to higher wing loading. Higher wing loading means more drag per span, and analogously, higher torques. For this reason, decreasing the diameter or increasing the thrust of a propeller decreases the propeller efficiency and increases the shaft power required to spin the propeller. Figure 8 shows diminishing returns for shaft power reduction as diameter increases because thrust is increasing linearly with diameter, while area increases with the square of diameter.

To understand the effect of tip Mach number, again consider a rotating wing. For a fixed wing geometry, the lift will increase with velocity, and similarly, the thrust will increase with rotational velocity. If the tip speed is decreased, then the thrust must come from more aggressive blade shaping, for instance, increasing the sectional lift coefficient from 1.0. The PEGASUS concept would benefit from raising the tip Mach number above 0.8. Advanced propeller design is beyond the scope of this work, but highly swept, scimitar blades would be able to operate at higher Mach numbers than those designed by XROTOR.

C. Thrust Distribution Between Propellers

A final study was undertaken to investigate the effect of splitting the required thrust across the inboard and wingtip propellers. The initial concept of operations for PEGASUS was to use only the wingtip propellers during cruise, but there are scenarios where operating the inboard propulsors may yield benefits. One scenario in particular is if the goal is to reduce emissions during the flight. Because the inboard motors are electrically powered, using the inboard motor in lieu of the wingtip propulsors should reduce emissions. Figure 9 shows the result of this study.

Within the figure, the x-axis is the percent of the total thrust being generated by the inboard propulsor class. Thus the left-hand side, at zero percent inboard thrust, implies all the thrust is generated by the tip propellers. Conversely, the right-hand side is a standard ATR-42-500 configuration in which all thrust is generate by the inboard propulsors. For this analysis, the inboard motors are placed at the same location as the ATR-42-500 engines, 20 ft from the aircraft centerline. An early study with the framework was the effect of the spanwise location of the inboard propeller, but as noted in Section II, Veldhuis and others have found a benefit to moving propellers toward the wingtip. In a similar fashion, when the location was not fixed, the optimizer always moved the inboard propulsor as far toward the wingtip as the constraints would allow. Therefore, rather than keep the location as a design variable, the inboard propeller location was fixed at the ATR-42-500 location.

The inboard propellers have six blades with a 13 ft diameter. The tip propellers also have six blades, but a diameter

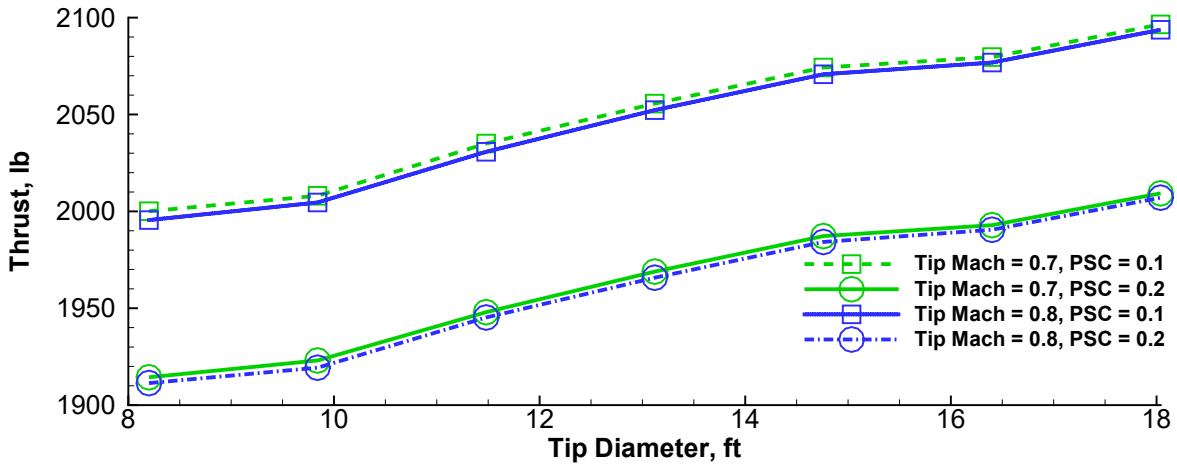

(a)

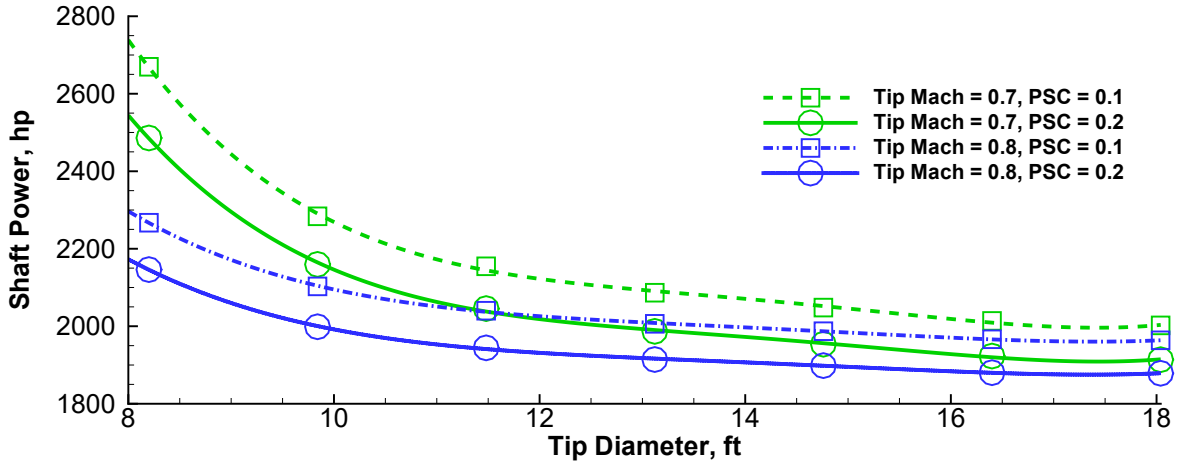

(b)

Fig. 8 Thrust and power required to maintain level flight using only the wingtip propeller. The target C_L is 0.5.

of 10.6 ft. This diameter was chosen because it results in only a small increase from the minimum power setting with a much reduced diameter. The analysis framework assumes NLF everywhere except aft of the propellers, and when the thrust is provided by only one propulsor class, the other propulsor class is removed from the computation. This would be representative of folded inboard propellers, or a standard configuration without a wingtip propeller.

The figure shows a general parabolic trend in shaft power, with dips at each extreme. The reason for the dips is the increased laminar flow that comes with "turning off" one propulsor class. The reason that the 100% inboard thrust configuration has a lower power consumption than the 100% tip configuration is the difference in propeller diameters. If the wingtip propeller diameter were increased such that it were larger than the inboard, the graph would be "slanted" the other direction. Regardless, the trend shows that operating both propeller classes leads to the lowest total required power by a small margin. In terms of percentage reduction, the minimum power is approximately 5% lower than using a single propulsor class. The two propulsor class benefit is explained by disc loading, as has been the case with most other results. By sharing the thrust load across four propellers, the disc loading drops and the propeller efficiency increases. This increase in propeller efficiency offsets the additional thrust required to overcome viscous drag.

Figure 9 also shows that operating only the wingtip propulsors reduces the required thrust compared with operating both classes, or the inboard propulsors alone. There is a small change from greatest thrust to least thrust, again approximately 5%. These trends come from the fact that larger propellers reduce the amount of laminar flow on the

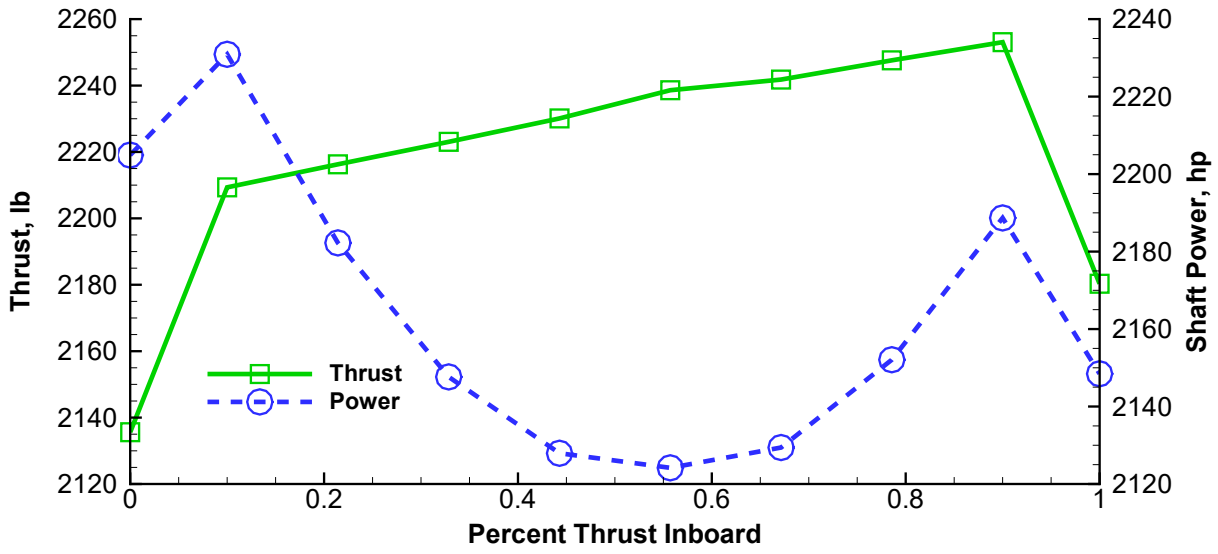

Fig. 9 Thrust and power required to maintain level flight as a function of thrust distribution between the two propulsor classes.

wing, and that the wingtip propellers are better suited at reducing the induced drag than the inboard propellers.

A final data point from this study comes from comparing the induced drag for the 100% inboard condition and the 100% wingtip condition against the clean wing configuration. FlightStream predicts a 9% decrease in induced drag by using a tip propulsor compared with a clean wing. Similarly, the program predicts a 5% induced drag reduction over the clean wing when the inboard motor is used, from which one can infer a 4% benefit from using the wingtip propulsor class over the inboard propulsor class. Although a 4% reduction in induced drag is a benefit, it constitutes a small portion of the total drag, whereas operating both propellers at a 50-50 power split essentially halves the disc loading. The reduction in disc loading more than compensates for the drag reduction, leading to the "power bucket" shown in Fig. 9. Obtaining a reduction in induced drag when using the inboard propeller is feasible given the initial wing was not optimized to minimize induced drag at the onset.

V. Concluding Remarks

This paper presented the propulsion-aerodynamic interference effects of multiple propellers across a wing. Using FlightStream, a surface vorticity solver with actuator discs that implement Conway's model, the effect of propeller slipstream on system power was estimated. The tools were validated against experimental data to show that FlightStream was capable of accurately modeling the aerodynamic performance of a wing in a propeller's slipstream. The analysis verified past results, showing that tip propellers can reduce the induced and total drag of a wing. The analysis also showed the importance of selecting the objective function by which a configuration is measured. When considering drag alone, smaller propellers are superior to larger propellers to create a low-drag, balanced flight configuration. However, smaller propellers lead to higher disc loading, which in turn leads to higher consumed shaft power. As a result of the high disc loading and corresponding low propeller efficiency for small propellers, the minimum power requirements come from large propellers.

Additional trades examined the impact of helical tip Mach number and power saving coefficient provided by the aft boundary layer propulsor. These trades further highlighted the impact of disc loading on propeller efficiency. In general, any modification to lower the disc or blade loading will improve the propeller efficiency and show significant system benefits. Though a detailed propeller design was not performed, common means of lowering blade loading include increasing the number of blades, increasing the tip speed, or increasing the propeller swept area. Adding additional propellers, such as the inboards or the aft BLI propulsor, increases the system disc area. For the sample analysis performed in this study, using the inboard motors in addition to the wingtip engines leads to a reduced system power consumption compared to using only one propulsion system.

VI. Future Work

The baseline PEGASUS concept borrows heavily from the ATR-42-500. This work, and the continuing effort on PEGASUS, strives to increase the analysis behind the design decisions driving the aircraft configuration. As such, additional analysis will continue to understand the potential benefits associated with the aft propulsor. The power saving coefficient will be replaced by a viscous computational fluid dynamic (CFD) model detailing the fuselage profile and an actuator disc. This enables the of modeling the boundary layer growth and how effectively the aft propulsor can re-energize the low-momentum flow.

Another area of improved fidelity comes from the wing design. The baseline wing followed the ATR-42-500 planform and an estimated airfoil shape. To improve on the integrated aspect of PAI, the wing and propulsors should be designed with one another in mind. At a minimum, this means investigating the twist distribution across the wing in the presence of the propeller slipstream.

Future work will also focus on on including the source of power. This work demonstrated the value of using multiple propellers during cruise using only the total shaft power required as a metric. The cost of generating that shaft power, which comes from a hybrid electric motor at the wingtip and battery inboard, may lead to a different optimium solution. For example, the battery energy density (kJ/kg) is significantly lower for batteries than it is for chemical fuels. Thus when optimizing on system weight, using the wingtip propulsor may be more favorable.

VII. Acknowledgments

The author would like to thank Francisco Capristan, Jesse Quinlan, and Mark Guynn for their guidance and input on the PEGASUS aircraft. This work was supported by the NASA Advanced Air Transport Technology (AATT) project.

References

[1] Antcliff, K. R., Guynn, M. D., Marien, T., Wells, D. P., Schneider, S. J., and Tong, M. J., "Mission Analysis and Aircraft Sizing of a Hybrid-Electric Regional Aircraft," AIAA SciTech Forum, American Institute of Aeronautics and Astronautics, 2016. doi:10.2514/6.2016-1028, URL https://doi.org/10.2514/6.2016-1028.

[2] Antcliff, K. R., and Capristan, F. M., "Conceptual Design of the Parallel Electric-Gas Architecture with Synergistic Utilization Scheme (PEGASUS) Concept," AIAA AVIATION Forum, American Institute of Aeronautics and Astronautics, 2017. doi:10.2514/6.2017-4001, URL https://doi.org/10.2514/6.2017-4001.

[3] Gray, J. S., Kenway, G. K., Mader, C. A., and Martins, J., "Aero-propulsive Design Optimization of a Turboelectric Boundary Layer Ingestion Propulsion System," AIAA AVIATION Forum, American Institute of Aeronautics and Astronautics, 2018. doi:10.2514/6.2018-3976, URL https://doi.org/10.2514/6.2018-3976.

[4] Kroo, I., "Propeller-wing integration for minimum induced loss," *Journal of Aircraft*, Vol. 23, No. 7, 1986, pp. 561–565. doi:10.2514/3.45344, URL https://doi.org/10.2514/3.45344.

[5] Veldhuis, L., "Review of Propeller-Wing Aerodynamic Interference," *24th International Congress of the Aeronautical Sciences*, 2004.

[6] Miranda, L., and Brennan, J., "Aerodynamic effects of wingtip-mounted propellers and turbines," Fluid Dynamics and Co-located Conferences, American Institute of Aeronautics and Astronautics, 1986. doi:10.2514/6.1986-1802, URL https://doi.org/10.2514/6.1986-1802.

[7] Ahuja, V., and Hartfield, R., "Predicting the Aero Loads Behind a Propeller in the Presence of a Wing Using Flightstream," AIAA AVIATION Forum, American Institute of Aeronautics and Astronautics, 2015. doi:10.2514/6.2015-2734, URL https://doi.org/10.2514/6.2015-2734.

[8] Conway, J. T., "Analytical solutions for the actuator disk with variable radial distribution of load," *Journal of Fluid Mechanics*, Vol. 297, 1995, pp. 327–355. doi:10.1017/s0022112095003120, URL https://www.cambridge.org/core/article/analytical-solutions-for-the-actuator-disk-with-variable-radial-distribution-of-load/DD0A601AF1DF77542B094AF6DDCD99EB.

[9] Sandoz, B., Ahuja, V., and Hartfield, R. J., "Longitudinal Aerodynamic Characteristics of a V/STOL Tilt-wing Four-Propeller Transport Model using a Surface Vorticity Flow Solver," AIAA SciTech Forum, American Institute of Aeronautics and Astronautics, 2018. doi:10.2514/6.2018-2070, URL https://doi.org/10.2514/6.2018-2070.

[10] Ahuja, V., Hartfield, R. J., and Burkhalter, J. E., "Optimizing Engine Placement on an Aircraft Wing using Bio-mimetic optimization and FlightStream^{TM}," AIAA SciTech Forum, American Institute of Aeronautics and Astronautics, 2017. doi:10.2514/6.2017-0235, URL https://doi.org/10.2514/6.2017-0235.

[11] Gabor, O. S., Koreanschi, A., and Botez, R. M., "Low-speed aerodynamic characteristics improvement of ATR 42 airfoil using a morphing wing approach," *IECON 2012 - 38th Annual Conference on IEEE Industrial Electronics Society*, 2012, pp. 5451–5456.

[12] ATR, "ATR 42-300/-320," , Jun. 2011. URL www.atraircraft.com/products_app/media/pdf/ATR_42-300-320.pdf.

[13] Jackson, P. (ed.), *IHS Jane's All the World's Aircraft*, IHS, 2016-2017.

[14] Hahn, A., "Application of Cart3D to Complex Propulsion-Airframe Integration with Vehicle Sketch Pad," Aerospace Sciences Meetings, American Institute of Aeronautics and Astronautics, 2012. doi:10.2514/6.2012-547, URL https://doi.org/10.2514/6.2012-547.

[15] Raymer, D. P., *Aircraft Design: A Conceptual Approach*, AIAA Education Series, 2012.

[16] Drela, M., "Power Balance in Aerodynamic Flows," *AIAA Journal*, Vol. 47, No. 7, 2009, pp. 1761–1771. doi:10.2514/1.42409, URL https://doi.org/10.2514/1.42409.

[17] Drela, M., and Youngren, H., "XROTOR Download Page," , Mar. 2011. URL http://web.mit.edu/drela/Public/web/xrotor/, accessed Nov. 2018.

[18] McCullers, L. A., "Aircraft Configuration Optimization Including Optimized Flight Profiles," *Recent Experiences in Multidisciplinary Analysis and Optimization*, edited by J. Sobieski, NASA, NASA, 1984, pp. 395–413.